Journal of Materials Chemistry B

Accepted Manuscript

ROYAL SOCIETY OF CHEMISTRY

www.rsc.org/materialsB

Understanding cell homing-based tissue regeneration from the perspective of materials

Dapeng Zhao,[a] Lei Lei, *[b] Shuo Wang[a] and Hemin Nie*[a]

[a] *Department of Biomedical Engineering, College of Biology, Hunan University, Changsha 410082, China*

b Department of Orthodontics, Xiangya Stomatological Hospital, Central South University, Changsha 410008, China

***Correspondence to:**

Hemin Nie, Ph.D., Professor

Department of Biomedical Engineering, College of Biology, Hunan University

Yuelu Mountain, Changsha 410082, China

Tel.: +86 731-83998487

Fax: +86 731-88821720

E-mail address: niehemin@hnu.edu.cn (H. Nie)

Lei Lei, M.D., Ph.D.

Department of Orthodontics, Xiangya Stomatological Hospital, Central South University

72 Xiangya Road, Kaifu District, Changsha 410008, China

Tel.: +86 731-82355112

Fax: +86 731-84805086

E-mail address: leilei8413@163.com (L. Lei)

Abstract:

Homing of cells to their target organs for tissue defect repair poses a significant challenge to biomaterials scientists and tissue engineers, due to the low efficiency of homing of effective cells to defect sites as well as the difficulties in coordinating cell migration, adhesion, spreading and differentiations. Recent advances in biomaterials have successfully improved the efficiency of homing of mesenchymal stem cells (MSCs) and cell homing-based tissue regeneration. In this review, the process of cell-homing based tissue regeneration was discussed from three different perspectives, including cell surface engineering, scaffold optimization and signaling molecules interactions. Cell surface modification by using polymeric materials offers a simple way to administrate cell migration. Besides, the ordered or anisotropic structures are proved to be more efficient for cell adhesion, spreading and infiltration than relatively random or isotropy structures. Moreover, the coordinated release of different growth factors (GFs), e.g. achieved via core-shell microspheres, can orchestrate the biological processes, including cell growth and differentiations, and significantly enhance the osteogenic differentiation of low population density of MSCs. These developments in biomaterials are not only important for fundamental understanding of materials-cell interactions, but also help understand cell homing-based tissue regeneration from the perspective of materials, which is crucial for the design and fabrication of a new generation of highly functional biomaterials for tissue regeneration.

1. Introduction

Incurable diseases always resulted in tissue defects in patients.[1-3] As an emerging treatment strategy, tissue engineering focuses on repairing damaged tissue and restoring tissue functions by employing three fundamental "tools", i.e., cells, scaffolds and growth factors (GFs).[4-6] There are two categories of approaches for tissue regeneration: cell transplantation and cell homing.[7-9] The former ones focus on introducing exogenous cells into the defect sites to heal tissue defects, while the latter approaches use biomaterials to induce the migration of the systemically transplanted cells or host cells to defect sites in an attempt to harness the potential of them in regenerating damaged tissues.[1, 10] Although local cell transplantation seems straight-forward, low efficiency of this strategy in repairing large tissue defects suggests that this kind of therapy doesn't harness the host's innate capacity for repair. As a promising alternative treatment to local cell transplantation, tissue regeneration by the localization of circulating cells (including host and/or systemically transplanted cells) has attracted increasing attention over past years.[11, 12]

A series of cytokines play roles in the homing of MSCs. For example, it has been reported that stromal-derived factor-1 (SDF-1) is an important chemokine, which determines the migration and homing of MSCs.[13-16] The recognition of chemokine SDF-1 during the homing of MSCs requires a key receptor, i.e., CXC chemokine receptor 4 (CXCR4).[17] Thus, the MSCs experienced *in vitro* cultivation, with down-regulated expression of CXCR4, showed an inefficient homing towards ischemic myocardium.[18, 19] On the other hand, the presence of relevant cell adhesion ligands can enhance cell homing.[18, 20, 21] For instance, Sarkar et al. modified the surface of mesenchymal stem cells (MSCs) with nano-sized polymer constructs containing sialyl Lewis^x,[22] which mediate cell rolling within inflamed tissue. It was found that the modified MSCs homed to the inflamed tissue with much higher efficiency than the MSCs without surface modification. These cell modification methods may help improve the efficiency of cell homing to tissue defect sites and make cellular preparation for cell proliferation and differentiations *in situ*.

An excellent scaffold not only provides a shelter for the homed cells, but also possesses the ability to regulate cellular functions, e.g. cell migration and differentiations.[6, 23] Therefore, the selection of biomaterials and the design of scaffolds have been widely studied.[24-27] Anatomically shaped human molar scaffolds and rat incisor scaffolds were produced via 3-dimentional printing.[28] The experimental results showed that the introduction of the growth factors (GFs), i.e., SDF-1 and bone morphogenetic protein-7 (BMP-7) into the microchannels of scaffolds led to significantly more recruited endogenous cells and greater angiogenesis compared with the GF-free scaffolds. Generally speaking, the dynamic interactions between cells and scaffolds determine various cellular functions, including cell adhesion, spreading, migration, infiltration and differentiation, which determine the fate of cells and the effectiveness of tissue repair.[29-32] In this sense, the proper application of biomaterials can maximize the positive influence of cell homing on tissue regeneration.[33]

A series of GFs participate and play different roles in the repair process of tissue defects, e.g. bone fractures. For instance, FGF-2 is one of the GFs that regulate cell growth and division.[34-36] As a prototype of bone morphogenetic proteins, BMP-2 induces the differentiation of mesenchymal stem cells into osteoblast precursors.[37] It has been shown that in the repair of bone defects or fractures, a combination of two or more GFs taking different roles or presenting in different stages in natural bone repair is advantageous over single growth factor.[38-43] In order to match the optimized microenvironment for tissue repair, a customized scaffold releasing multiple GFs in special pattern is warranted.[44, 45]

As suggested above, each of the three components of cell homing-based tissue engineering (**Fig. 1**) can be improved by taking full advantage of biomaterials.[46-49] In this review, each of the components has been considered from the perspective of materials. Throughout the text, these considerations and their implications for cell homing-based tissue engineering will be explored.

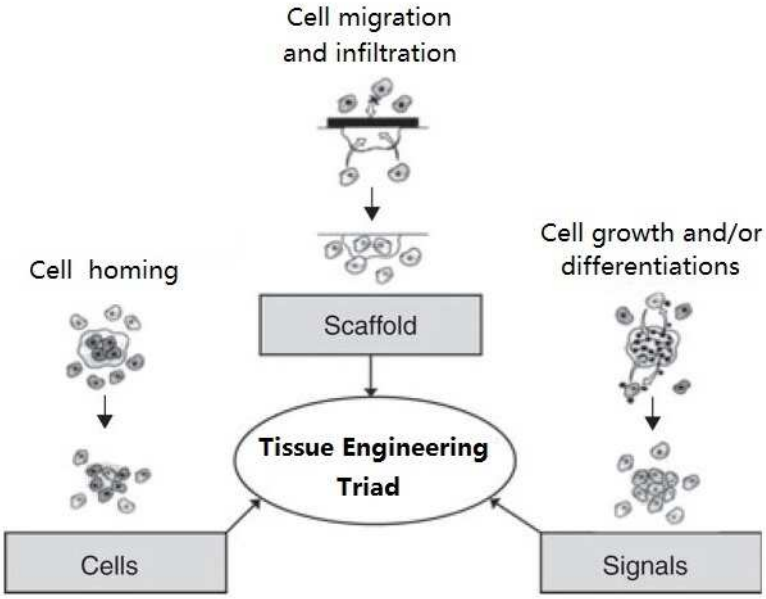

Fig. 1 The triad of cell homing-based tissue engineering. The three main design components in cell homing-based tissue engineering are based on the three main components of tissues: cells, their extracellular matrix (scaffolds) and a signaling microenvironment. Each of these components can be improved individually or in combination to optimize the regeneration of a damaged tissue via cell homing.

2. Improvement of cell migration by cell surface engineering

Previous investigations revealed that cell migration is regulated by a cooperation of homing ligand and chemokine receptor expressed on circulating cells.[50, 51] As described above, the recruitment of CXCR4+ MSCs to the SDF-1 gradient is very important for MSCs migration.[52-54] Consequently, the strategies, which can up regulate CXCR4 on cell surface, may result in more efficient homing of MSCs. The surface modification of living cells with polymers offers new opportunities in cell homing.[55] Generally speaking, there are three methods which have been applied for the surface modification of cells: (a) covalent conjugation; (b) hydrophobic interaction; and (c) electrostatic interaction [56]. Won et al. used lipid-PEG, which can provide a homogenous ultra-thin coating on cell surface, to improve the homing of MSCs to the ischemic myocardium.[57] DMPE-PEG was used to introduce recominant CXCR4 (rCXCR4) on the surface of MSCs in this investigation.

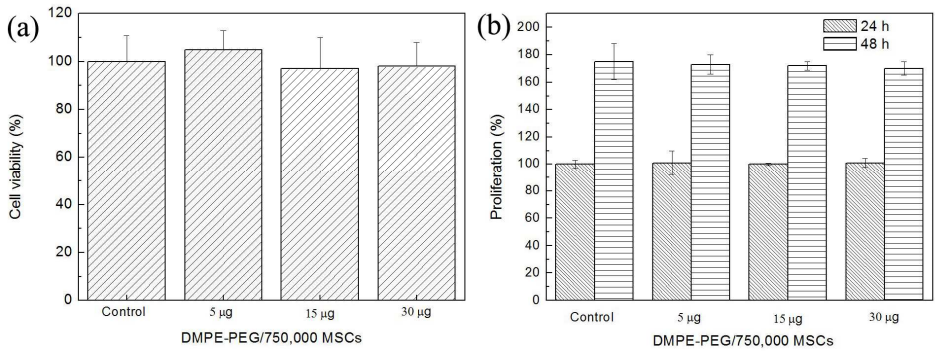

Fig. 2 (a) Cytotoxicity of the DMPE-PEG during incubation time of 48 h and (b) proliferation of the modified MSCs.

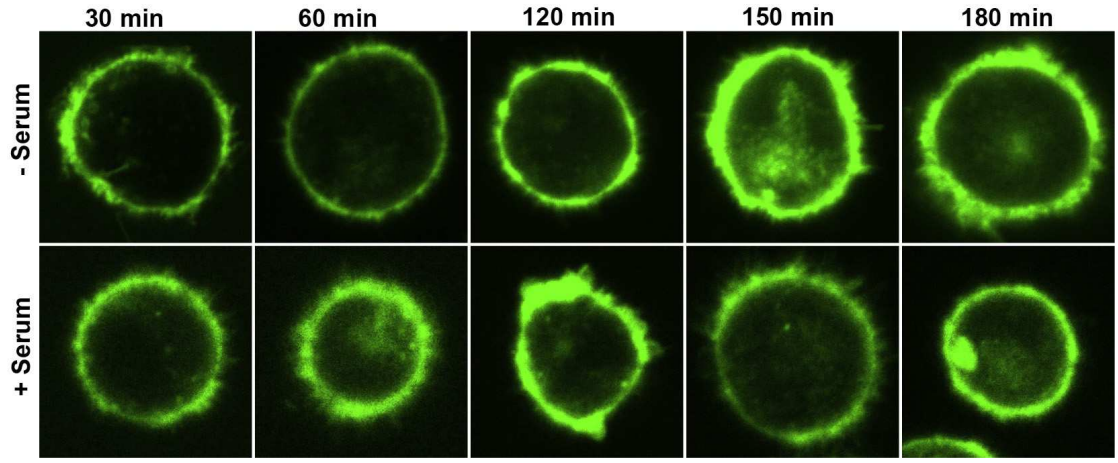

Fig. 3 The confocal micrographs of the DMPE-PEG on the surface of MSCs at various time points in the presence or the absence of human serum (reprinted with permission from Ref. 57. Copyright 2015, Elsevier, License No. 3671070999125).

The results of DMPE-PEG modification showed that DMPE-PEG was incorporated within the membrane of MSCs within only 2 min, and only a small amount of DMPE-PEG was required to modify a large number of MSCs, e.g. only 1 μg of the DMPE-PEG was enough for modifying 750,000 MSCs. In addition, the influence of the DMPE-PEG modification on MSC functions was investigated. **Fig. 2** presents the cell viability and proliferation rate of MSCs incubated with the DMPE-PEG (30μg/750,000 MSCs). Both cytotoxicity and proliferation results revealed that there was no obvious side effects of the DMPE-PEG on MSC adhesion. In order to investigate how long the DMPE-PEG stayed immobilized on the surface of the MSCs in serum, the FITC-labeled DMPE-PEG-immobilized MSCs were incubated for up to 180 min in the presence or the absence of 20 % human serum, and a confocal microscope was applied to locate the immobilized DMPE-PEG. **Fig. 3** revealed that

the DMPE-PEG was always detectable from 30 min up to 180 min, regardless of serum.

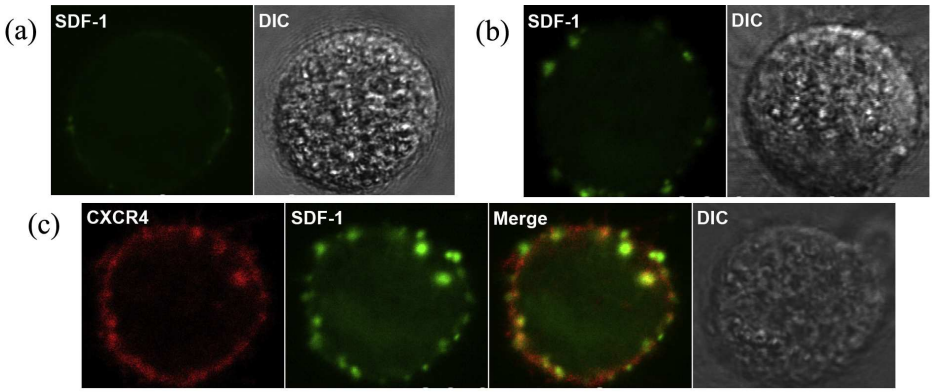

Fig. 4 The confocal micrographs of the MSCs surface of (a) the group of control + FITC-SDF-1; (b) the group of DMPE-PEG-CXCR4 + FITC-SDF-1; (c) the group of DMPE-PEG-R -CXCR4 + FITC-SDF-1 (reprinted with permission from Ref. 57. Copyright 2015, Elsevier, License No. 3671070999125).

A detailed study on the surface modification of MSCs with rCXCR4 was performed by conjugating rCXCR4 with the DMPE-PEG, followed by incubation with MSCs for 2 min. The confocal micrograph revealed that the rCXCR4-positive MSCs population was nearly 100 %. In order to verify the binding of recombinant SDF-1 (rSDF-1) with rCXCR4 on the surface of the MSCs, the MSCs were modified with the DMPE-PEG-FITC-Rho-CXCR4 (rhodamine labeled rCXCR4 conjugated with the DMPE-PEG) or the DMPE-PEG-CXCR4, followed by incubating with the labled rSDF-1 (FITC-SDF-1). **Fig. 4** presents the SDF-1 binding with CXCR4 on the surface of a MSC. In **Fig. 4b**, the group (CXCR-4+FITC-SDF-1) showed SDF-1 binding to the surface of the MSCs. In **Fig. 4c**, the co-localization of SDF-1 and CXCR4 on the cell surface was confirmed as well. By comparing **Fig. 4b and c**, it can be concluded that rhodamine did not influence the interaction between SDF-1 and CXCR4. In the normal MSCs group (Control + FITC-SDF-1, see **Fig. 4a**), the intensity of SDF-1 on cell surface was very low, indicating the low expression of CXCR4 in the MSCs post culture expansion.

Chang et al. reported that the number of circulating stem cells correlated positively with the circulating levels of SDF-1.[58] Kucia et al. revealed that with higher levels of

SDF-1 release after myocardial infarction, more stem cells were found to release from the bone marrow to the peripheral blood.[59] In addition, it has been reported that the binding of SDF-1 with CXCR4 can lead to the activation of multiple downstream signaling pathways in targeted cells, and thus can regulate the biological effects regarding cell motility, cell adhesion and chemotactic responses.[60] The study of Won and coworkers[57] confirmed the dependence of the migration of CXCR4+ MSCs toward SDF-1 on the concentration of SDF-1, as well as on the dose of CXCR4 modified on the surface of MSCs.

These results indicate that stem cell homing can be improved by modifying the surface of cells with polymers conjugated with receptors, leading to the recruitment of correct and enough seed cells into tissue defect sites.

3. Improvement of cell migration and infiltration by using scaffolds with ordered-structures

The design of scaffolds with tissue-specific structures is important for tissue repair.[61] It has been revealed that the three-dimensional structures of a scaffold, including porosity, pore size, pore morphology and orientation, have significant influence on the mechanical behavior and biocompatibility.[62-67] However, most current scaffolds exhibited random structures, which can't facilitate the easy migration and infiltration of the homed cells. Therefore, the design and fabrication of scaffolds with ordered-structures has received increasing attention over the past years.

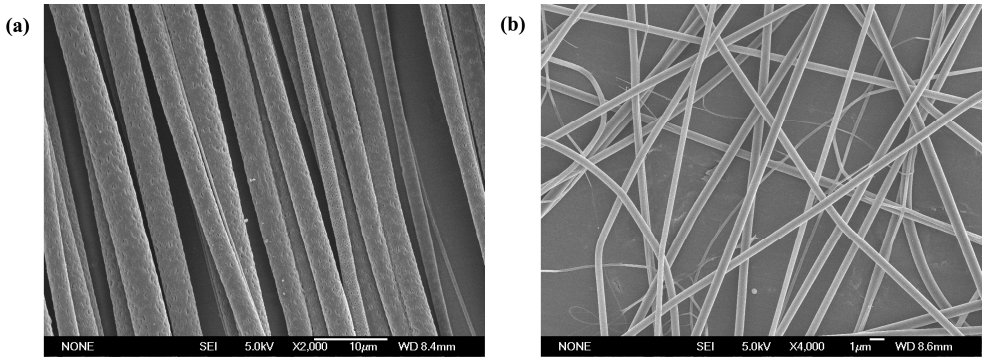

Fig. 5 SEM micrographs showing (a) aligned electrospun PCL-gelatin ultrafine fibers and (b) non-aligned electrospun PCL-gelatin ultrafine fibers.

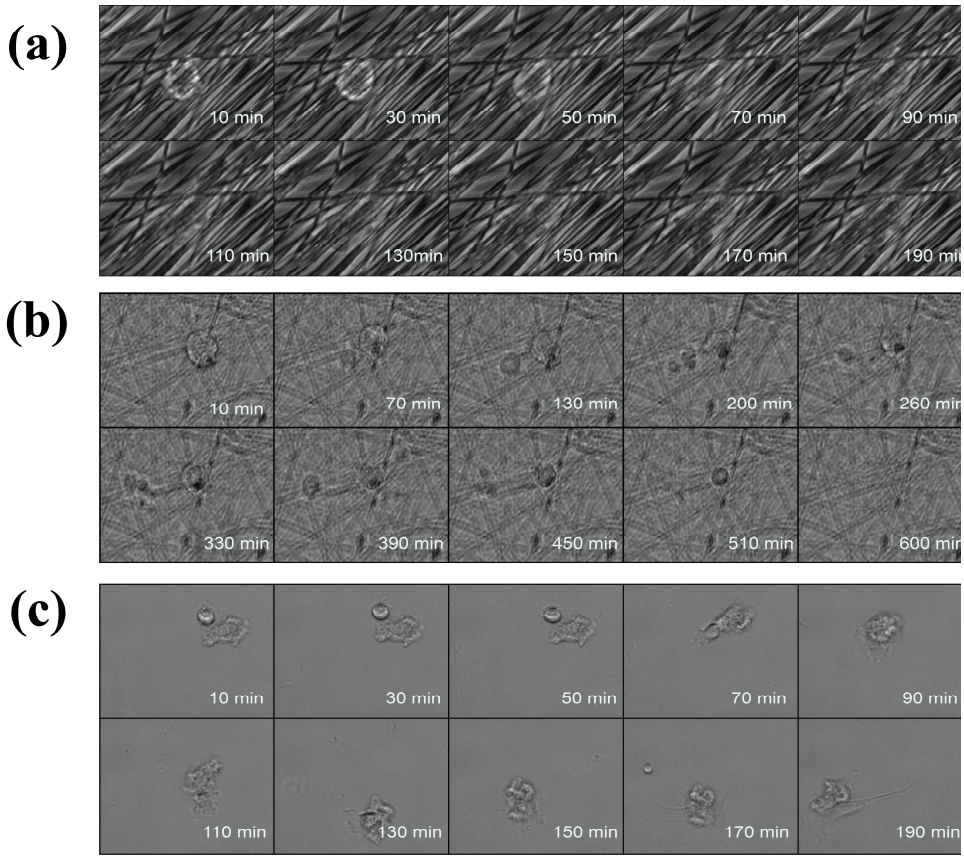

Fig. 6 Time-lapse microscopy images of the dynamic spreading and morphological changes of MSCs after seeding on (a) aligned fibers, (b) non-aligned fibers and (c) glass coverslips. Dotted yellow circles show the location of the cells of interest on two kinds of fibrous scaffolds. Scale bar = 20 mm (reprinted with permission from Ref. 71. Copyright 2015, Royal Society Chemistry, License No. 3671171281671).

3.1. Electrospun ultrafine fibers

Electrospinning is a simple and inexpensive method to fabricate ultrafine polymer fibers.[68, 69] Unnithan et al. reported that electrospun fibers have attracted increasing interest for tissue engineering applications including bone, cartilages, muscles, skin and blood vessels.[70] However, the understanding of dynamic interactions between cells and electrospun fibers is still limited. Wang et al. produced aligned and non-aligned electrospun PCL-gelatin ultrafine fibers using the electrospinning method, and examined the interactions between them and mesenchymal stem cells (MSCs) using time-lapse microscopy.[71] PCL–gelatin solution (concentration: 10 wt. %) was transferred to a 5 ml glass syringe fitted with a 27 g needle and delivered at a flow rate of 1.0–1.5 ml/h. The flow was ejected at a voltage of 8–10 kV. Aligned ultrafine

fibers were collected on a glass coverslip attached on a rotating disk (1000 rpm). While, non-aligned ultrafine fibers were collected using a 15 mm-diameter glass coverslip placed on a static flat collector. **Fig. 5** presents the SEM images of both aligned and non-aligned electrospun ultrafine fibers. The aligned fibers showed a high level of alignment, but the non-aligned fibers were dispersed randomly.

The real-time interactions between the aligned/non-aligned fibers and MSCs were tracked using time-lapse phase contrast microscopy. **Fig. 6** shows the initial cell attachment and spreading after seeding. The cells on aligned fibers, gradually spreading along the direction of the alignment, exhibit an elongated shape. The fully spread of these cells took less than 4 h. In contrast, the cells on non-aligned fibers extended along all directions and maintained the round shape. The time of spreading on non-aligned fibers was around 10 h. **Fig. 7** presents the tracks of the migration of individual cells on various materials as well as the corresponding summarized trajectories of around 20 MSCs. A highly consistent movement of cells along the fiber alignment direction was observed on aligned fibers (see **Fig. 7d**), but the motility on non-aligned fibers was random (see **Fig. 7e**). The migration of MSCs was further investigated by placing the 6-well plates (with MSCs seeded on different materials) at an angle of 45 °. **Fig. 8** shows the crystal violet staining results, revealing that the MSCs migrated out of the place where they were seeded on both aligned and non-aligned fibers, but the migration speed on the former material was significantly higher than on the latter. To sum up, aligned fibers significantly enhanced the spreading and migration of MSCs compared with the cells seeded on non-aligned fibers. Consequently, aligned ultrafine fibers can be a promising candidate scaffold providing enhanced cell-materials interactions.

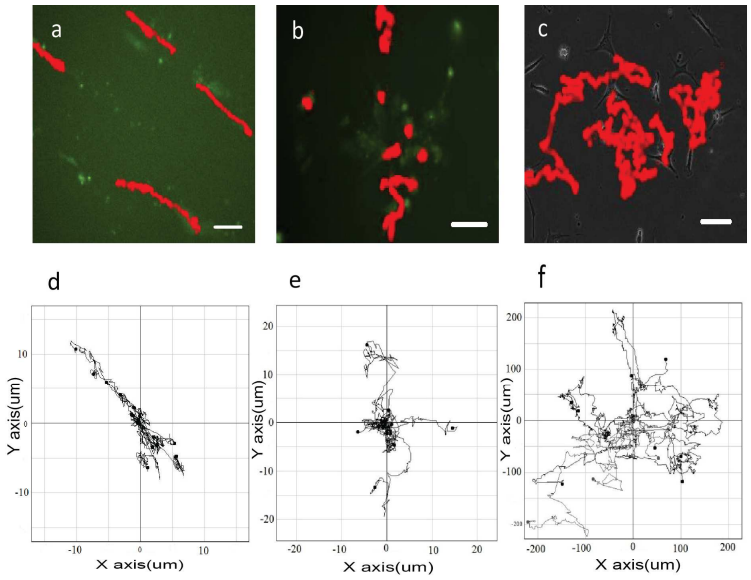

Fig. 7 The tracks of cell migration and the summarized trajectories of cells on aligned fibers (a), non-aligned fibers (b) and glass coverslips (c). (d–f) show summarized cell trajectories of cells on corresponding substrates (a–c). Scale bar: 5 mm (a); 10 mm (b); 50 mm (c) (reprinted with permission from Ref. 71. Copyright 2015, Royal Society Chemistry, License No. 3671171281671).

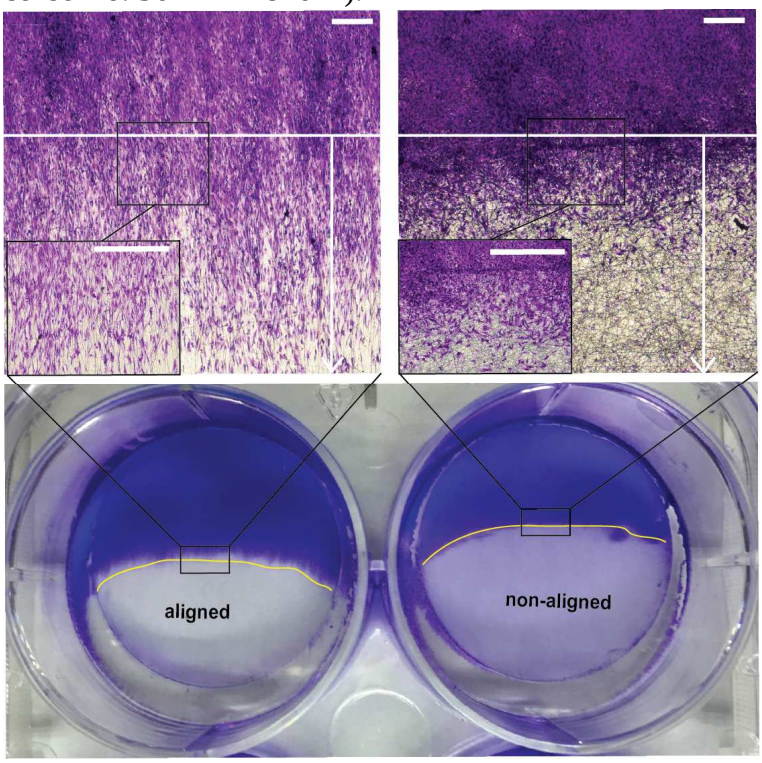

Fig. 8 Representative optical images of cell migration on aligned and non-aligned fibers. Scale bar: 50 mm (reprinted with permission from Ref. 71. Copyright 2015, Royal Society Chemistry, License No. 3671171281671).

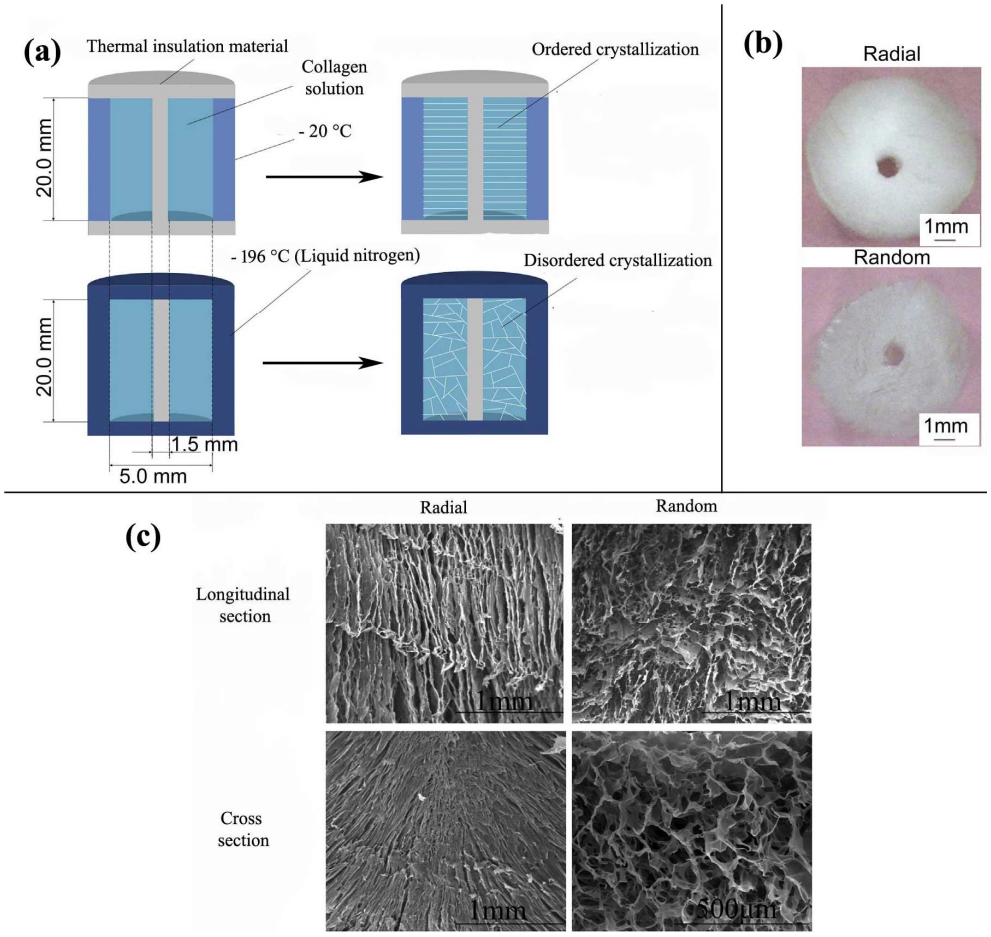

Fig. 9 Macroscopic and microscopic structures of the collagen scaffolds. (a) Fabrication of the radially oriented and random collagen scaffolds. (b) Microscopic structure of the collagen scaffolds (reprinted with permission from Ref. 72. Copyright 2015, Elsevier, License No. 3671211401420).

3.2. Radially oriented collagen scaffold

A radially oriented collagen scaffold was designed in order to meet the critical need of satisfactory outcomes in cartilage repair.[72] **Fig. 9** presents the fabrication as well as the macroscopic and microscopic structures of the radially oriented collagen scaffolds, with randomly oriented ones as control. The radially oriented scaffolds were produced using a temperature gradient-guided thermal-induced phase-separation technique. As shown in **Fig. 9a**, the collagen solution (dissolved in acetic acid, 10 mg/ml) was added to a mold with copper wall (-20 °C) but thermal insulation plastic top and bottom. During the evaporation of the liquid nitrogen, the collagen solution was unidirectionally frozen from the edge to the center of the solution. While, random collagen crystallization occurred in a mold stayed in liquid nitrogen (-196 °C, 10 min).

Fig. 9b reveals that the radially oriented scaffolds have oriented channels in both the horizontal and the vertical directions. Since the stimulation effects of SDF-1 on stem-cell homing[54] and migration[73] has been demonstrated, SDF-1 was introduced into the radially oriented scaffolds. Radially oriented or random scaffolds with or without SDF-1 were immersed in medium with suspensions of bone marrow stromal cells (BMSCs) to investigate the influence of different scaffolds on cell migration. **Fig. 10** shows that more cells were observed in radially oriented scaffolds than in random ones and the largest number of BMSCs was observed in the radially oriented scaffolds with SDF-1 (see **Fig. 10a**). Similar results were observed in the cell counting kit-8 (CCK-8) assays as shown in **Fig. 10b**. These results suggested that the radially oriented scaffolds could promote BMSCs migration, and the addition of SDF-1 could further enhance this effect.

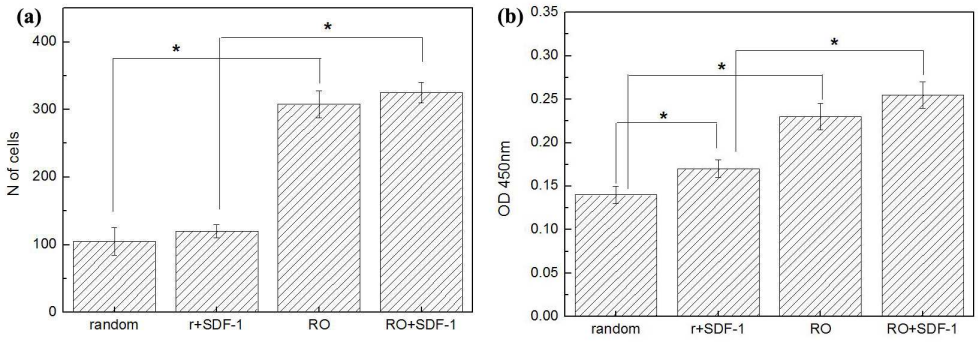

Fig. 10 Radially or random oriented collagen scaffolds with or without SDF-1 facilitates the migration of BMSCs. (a) Cell number; (b) CCK-8 assays of scaffolds with or without SDF-1. (r+SDF-1: random scaffold with SDF-1; RO: radially oriented scaffold without SDF-1; RO+SDF-1, radially oriented scaffold with SDF-1.) *p < 0.05 (ANOVA).

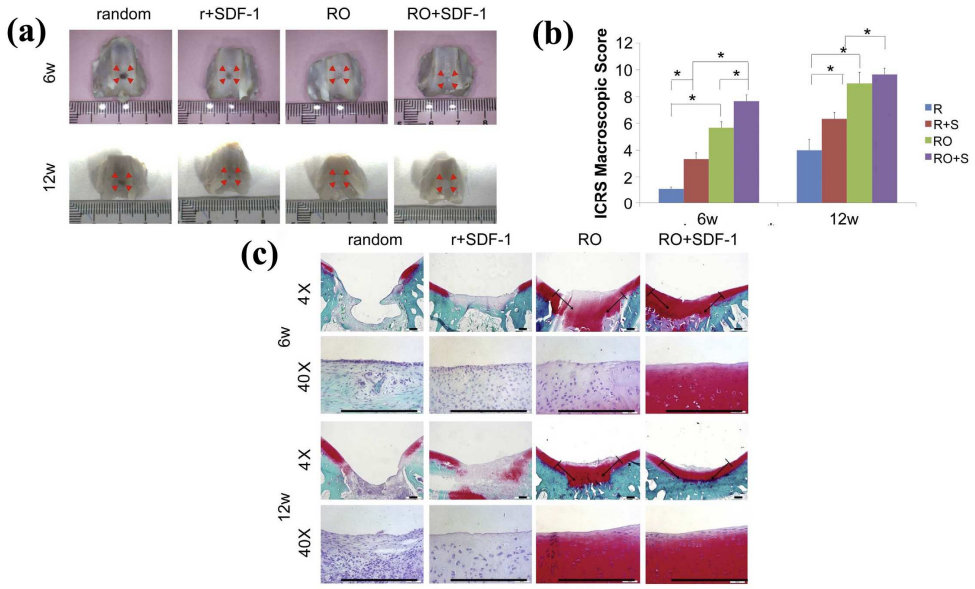

Fig. 11 Radially oriented collagen scaffold with SDF-1 for *in vivo* cartilage regeneration. (a) Gross findings with healed defects indicated by red arrows. (b) Macroscopic evaluation according to ICRS macroscopic scores. (c) Safranin-O staining images. The lines indicate the defect edges, and the arrows indicate the tissue protruding. Scale bars, 250 mm. *$p < 0.05$ (ANOVA) (reprinted with permission from Ref. 72. Copyright 2015, Elsevier, License No. 3671211401420).

Further investigation focused on the effects of the radially oriented scaffolds on cartilage regeneration *in vivo*. Radially or randomly oriented collagen scaffolds with or without SDF-1 were transplanted into rabbit osteochondral defects. **Fig. 11a** shows that six and twelve weeks post surgery, only a soft and friable tissue was observed in random scaffolds. In contrast, the defects in radially oriented and radially oriented+SDF-1 groups had become firm and smooth. ICRS scoring results (**Fig. 11b)** also revealed that the efficacy of the radially oriented scaffold on cartilage regeneration had been significantly enhanced by the addition of SDF-1 (six weeks post surgery). The histological results of the repaired tissue at six weeks (shown in **Fig. 11c**) revealed that the joint surface of the defect in the radially oriented+SDF-1 group was smooth, and a mixture of fibrocartilage and cartilage-like tissue was observed. In contrast, only fibrous tissue was found in the joint surface of the defect in the random and random+SDF-1 groups. Moreover, twelve weeks post surgery, the joint surface of the defect in the random and random+SDF-1 groups were still filled with fibrous tissue instead of cartilage. While, thick, hyaline cartilage-like tissue was

observed in the joint surface of the defect in the radially oriented and radially oriented+SDF-1 groups. Considering both *in vitro* and *in vivo* data, it is reasonable to conclude that the radially oriented scaffolds, exhibiting ordered and aligned channels in both the horizontal and the vertical directions, can promote the homing of BMSCs to the cartilage defect and thus are beneficial to the osteochondral regeneration, which can be further enhanced by introducing SDF-1.

3.3. Three-dimensionally printed scaffolds

Three-dimensional (3-D) printing technology is an additive manufacturing technique using a layer-by-layer process to build objects, so it can fabricate scaffolds with structures that have the spatial features of native tissues.[74-76] Metallic, ceramic and polymer scaffolds with ordered 3-D structure have been successfully produced via 3-D printing technique.[77-83]

Recently, Xu et al. investigated the attachment and proliferation of MC3T3 cells on hierarchically porous nagelschmidtite (NAGEL) bioceramic composite scaffolds with various pore morphologies fabricated by using 3-D printing technique.[84] Fig. 12 shows the optical microscopy and SEM micrographs of the NAGEL scaffolds with varied macropore morphologies. It can be seen that the NAGEL scaffolds had well-controlled pore morphologies (square, triangle and parallelogram), and the pore size was about 500-1000 μm. Besides, the surface morphology of the macropore walls was smooth. The attachment rates and proliferation of MC3T3 cells on the NAGEL scaffolds and the porous β-tricalcium phosphate (β-TCP) scaffolds, which were used for comparison, are presented in Fig. 13. For all groups, the attachment rates were over 70 %, and no significant difference was observed between them. The MTT analysis shown in Fig. 13b revealed that the proliferation of MC3T3 cells on NAGEL scaffolds with triangular and parallelogram structures was higher than that on the β-TCP scaffolds, indicating that the 3-D printed NAGEL scaffolds may have improved osteogenic activity compared with β-TCP scaffolds. In addition, the proliferation of MC3T3 cells on NAGEL scaffolds with triangular and parallelogram

structures was slightly higher than that on square group. Such a difference suggested that the pore morphology is important for the cell response, which is in accordance with other investigations.[30, 85-87]

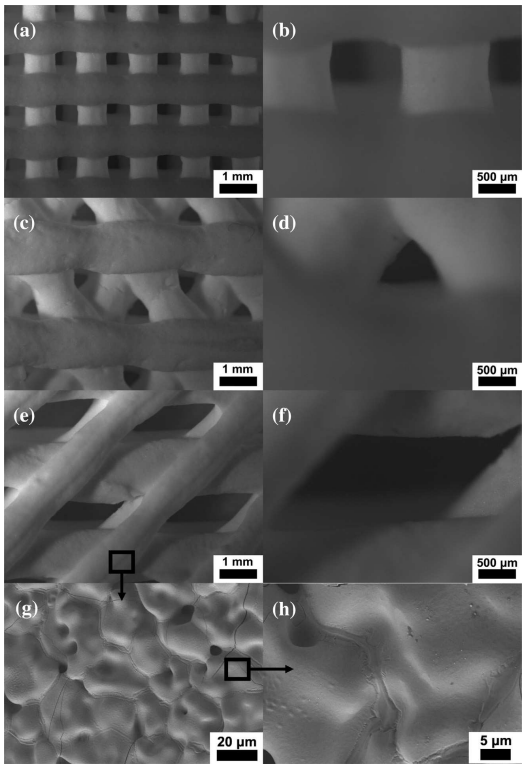

Fig. 12 Micrographs of 3-D plotted NAGEL scaffolds with (a, b) square, (c, d) triangular and (e, f) parallelogram pore structures. (g, h) Microstructure of the large pore walls. (b, d, f, h) Higher magnification images. The sizes of the macropores are about 500 – 1000 μm (reprinted with permission from Ref. 84. Copyright 2015, Elsevier, License No. 3671860733217).

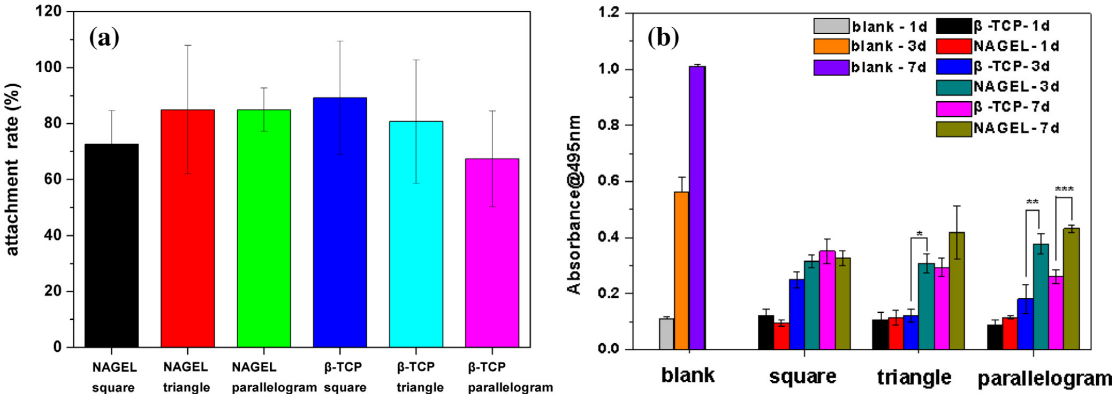

Fig. 13 (a) The rate of attachment of MC3T3 cells to 3-D plotted NAGEL scaffolds and b-TCP scaffolds with varied macropore structures. (b) The proliferation of 3T3 cells after culture on NAGEL and b-TCP scaffolds. ∗Significant difference ($p < 0.05$)

between the NAGEL and b-TCP triangular groups on day 3; **significant difference ($p < 0.05$) between the NAGEL and b-TCP parallelogram groups on day 3; ***significant difference ($p < 0.05$) between the NAGEL and b-TCP parallelogram groups on day 7 (reprinted with permission from Ref. 84. Copyright 2015, Elsevier, License No. 3671860733217).

4. Improvement of cell proliferation and differentiation by using core-shell microsphere

One of the key technical difficulties in cell homing-based tissue regeneration is how to take full advantage of the homed stem or progenitor cells in consideration of their low population density *in situ*. A high number of cells are considered advantageous if the repair of a large-sized tissue defect is concerned.[88] In this sense, how to coordinate cell proliferation and differentiation is a core challenge. Since a series of GFs demands different time scales and concentration profiles during a repair process, a programmed release of GFs is necessary.[89] Nevertheless, most delivery systems in the modern design only accounts for a single factor, limiting the overall efficacy of the therapy.[90, 91] Polymeric core-shell microspheres, synthesized by coaxial electrohydrodynamic atomization (CEHDA), were first reported by Nie and coworkers in 2010.[89] The double-wall structure of the microspheres allows the encapsulation of two different drugs at different compartments in one single step, which can lead to sequential or coupled release of drugs.[92] **Fig. 14** presents the schematic diagram showing the set of the CEHDA for core-shell microspheres fabrication. Poly (L-lactide acid) (PLLA, M_w = 85,000 – 160,000) and poly(D,L-lactide-*co*-glycolide acid) (PLGA, lactide/glycolide molar ratio = 50:50, M_w = 40,000 – 75,000) were selected as the core and shell of the core-shell microspheres, respectively. Two syringe pumps delivered the two kinds of polymer solutions at a specific rate into the inner and outer capillary of the coaxial needle. By changing the nozzle voltage (V_{nozzle}) and ring voltage (V_{ring}), a stable Taylor cone jet can be visually observed. A petri dish filled with anhydrous ethanol was used to collect the microspheres, so as to avoid the agglomeration of the microspheres. **Fig. 15** shows typical micrographs of the core-shell microspheres processed by CEHDA. According

to the SEM images in **Fig. 15a**, the microspheres show smooth surface and uniform size distribution. In addition, the core-shell structures were confirmed by a confocal microscope (see **Fig. 15b**).

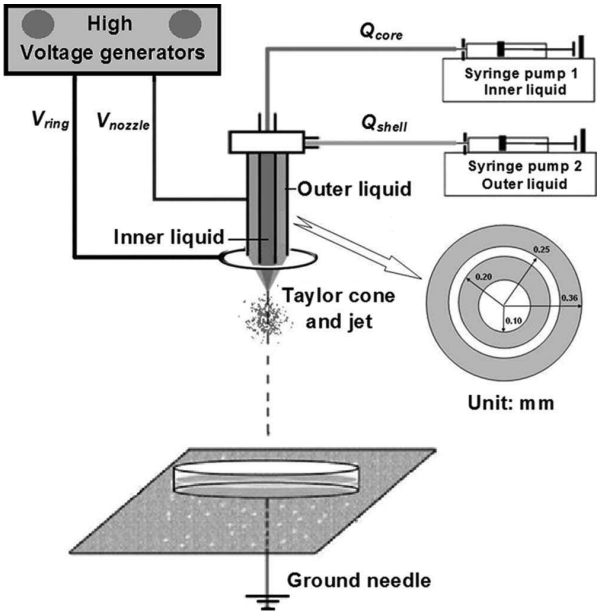

Fig. 14 Schematic diagrams depicting the set-up of coaxial electrohydrodynamic atomization (CEHDA). V_{nozzle} and V_{ring} are 6.5 KV and 3.5 KV, respectively, in a typical fabrication (reprinted with permission from Ref. 89. Copyright 2015, John Willey and Sons, License No. 3671250306434).

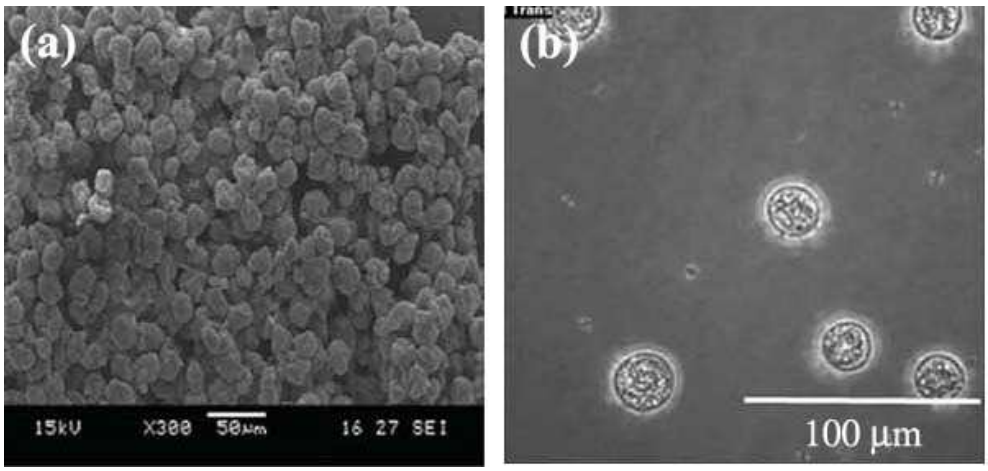

Fig. 15 Microstructures of core-shell microspheres fabricated by CEHDA. (a) SEM image; (b) confocal microscope image (reprinted with permission from Ref. 93. Copyright 2015, John Willey and Sons, License No. 3671631031732).

Table 1 Definition and configuration of experimental groups in *in vitro* release study and osteogenic induction assay.

Groups	Abbreviation	Description

Control	Ctrl	No microspheres
Blank 1	B1	Blank uniform microspheres
Blank 2	B2	Blank core–shell microspheres
Uniform	U	Dual GFs evenly distributed in uniform microspheres
FGF-2	F	FGF-2 evenly distributed in core and shell of microspheres
BMP-2	B	BMP-2 evenly distributed in core and shell of microspheres
Parallel	P	Dual GFs evenly distributed in core and shell of microspheres
Sequential 1	S1	FGF-2 solely distributed in core of microspheres; BMP-2 solely distributed in shell of microspheres
Sequential 2	S2	BMP-2 solely distributed in core of microspheres; FGF-2 solely distributed in shell of microspheres

Recently, the release patterns of FGF-2 and BMP-2 in different core-shell microspheres were characterized *in vitro* and *in vivo*.[93, 94] Lei et al. focused on the osteogenic response of low-population density of human MSCs (hMSCs) to various microspheres, including control (C), blank 1 (B1), blank 2 (B2), uniform microspheres (U), FGF-2 microspheres (F), BMP-2 microspheres (B), parallel microspheres (P), sequential 1 microspheres (S1) and sequential 2 microspheres (S2).[93] The detailed description of the experimental groups is presented in **Table 1**. Owing to the different positioning of GFs in various microspheres, various percentage release profiles were obtained (see **Fig. 16**). Because of the uniform structure and even distribution of FGF-2 and BMP-2 in the microspheres, the release of the GFs from group U was parallel. However, different release patterns of two GFs were observed in the core-shell microspheres. For instances, in the first week, only 15 % of FGF-2 but around 85 % of BMP-2 were released from the group S1, then the release of FGF-2 sped up and the release of it at day 30 was more than 85 %. Similarly, the group S2, i.e., the microspheres with core and shell with FGF-2 and BMP-2, respectively, released around 95 % of FGF-2 but less than 10 % of BMP-2 after 7 days. At day 30, the release of BMP-2 was around 88 %.

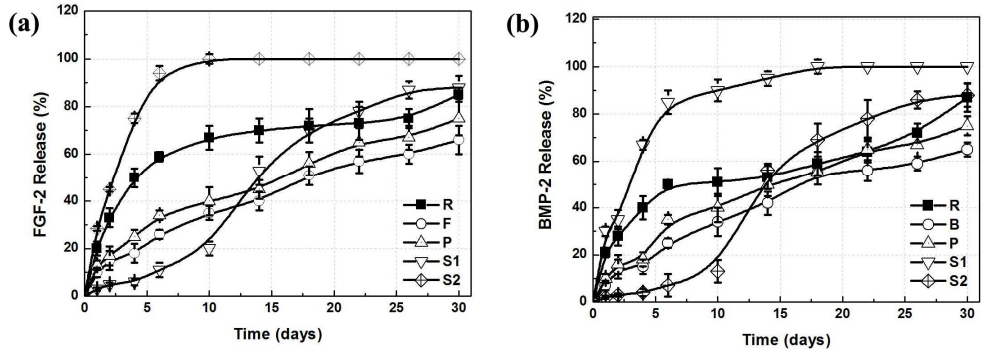

Fig. 16 Characterization of the *in vitro* release of (a) FGF-2 and (b) BMP-2 from various microspheres (reprinted with permission from Ref. 93. Copyright 2015, John Willey and Sons, License No. 3671631031732).

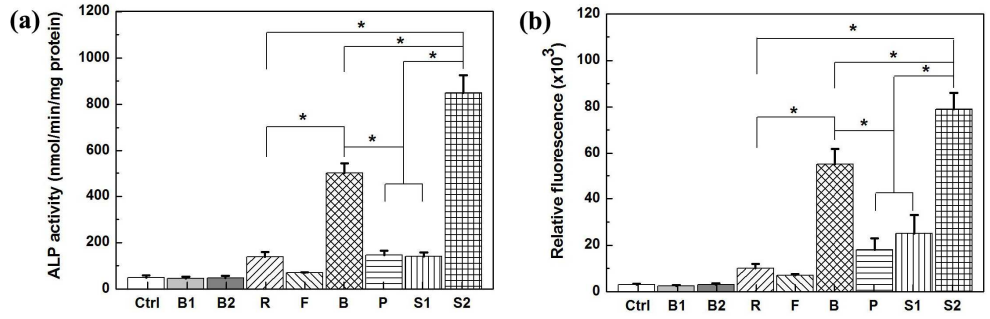

Fig. 17 Osteogenic differentiations of low-population density hMSCs induced by various microspheres for 4 weeks. (a) Quantification of ALP activity in hMSCs treated with various microspheres. (b) Quantification of calcium accumulation in hMSCs treated with various microspheres. Quantitative values are expressed as mean ±SD of six determinations (in triplicate each). *$p < 0.05$ (reprinted with permission from Ref. 93. Copyright 2015, John Willey and Sons, License No. 3671631031732).

In order to evaluate the osteogenic induction of low-population density of hMSCs by different microspheres, ALP activity and calcium concentration were analyzed as shown in **Fig. 17**. Albeit group S1 showed similar release pattern as group S2, the latter showed significantly higher ALP activity and calcium concentration. According to **Table 1** and **Fig. 16**, the only difference between S1 and S2 was the position and release sequence of FGF-2 and BMP-2. Consequently, the different osteogenic induction results between the two groups demonstrated that the release sequence of the two GFs was critical. As illustrated by Martin et al.,[95] FGF-2 can be viewed as a proliferative agent. However, BMP-2, a potent osteoinductive agent, can interfere the proliferation effect of FGF-2 by driving hMSCs to differentiate toward the osteogenic lineage.

In order to further evaluate the influence of the microspheres listed in **Table 1** on the bone regeneration, a rat tibia defect model was used.[94] A 2.5 mm long tibia fragment on the right side of a rat was cut out, followed by frozen in liquid nitrogen for 20 min. The fragment was then put back to its original site in the tibia and fixed perfectly on both ends. With the exception of the control group (group C), 20 mg of different microspheres was positioned next to the bone graft before the wound was closed with nylon sutures. In this case, the bone grafts would work as inorganic scaffolds for mechanical support and cell intrusions. So the intrusion of bone cells and formation of blood vessels in the bone grafts can reflect the degree of bone regeneration.

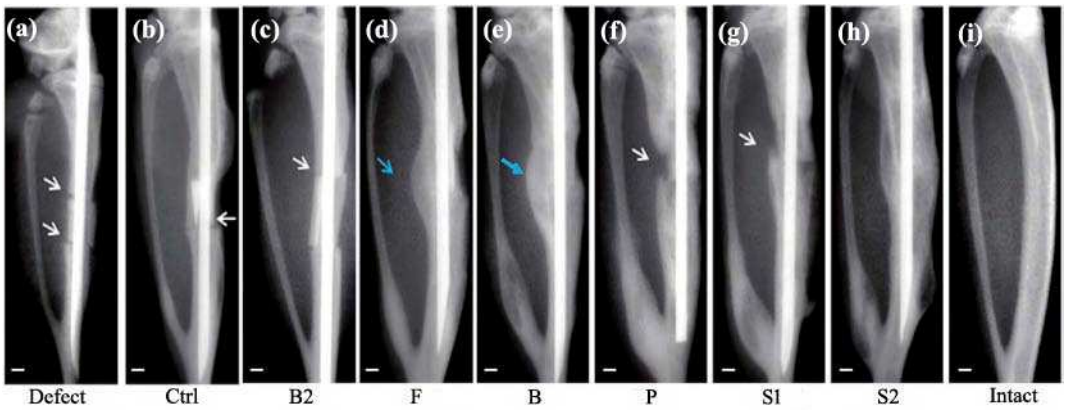

Fig. 18 Radiography of bone bridging after 4 weeks of different treatments in a critical-sized rat bone graft model. Radiographs of a rat tibia immediately after surgery (a), intact bone (i) and rat tibiae after 4 weeks of varied treatments (b–h) (refer to **Table 1**), with intact contralateral tibiae (left tibiae) denoted as a positive control. The white and blue arrows denote the bone defects and callus, respectively. Scale bar: 1 mm (reprinted with permission from Ref. 94. Copyright 2015, Royal Society of Chemistry, License No. 3671210677399).

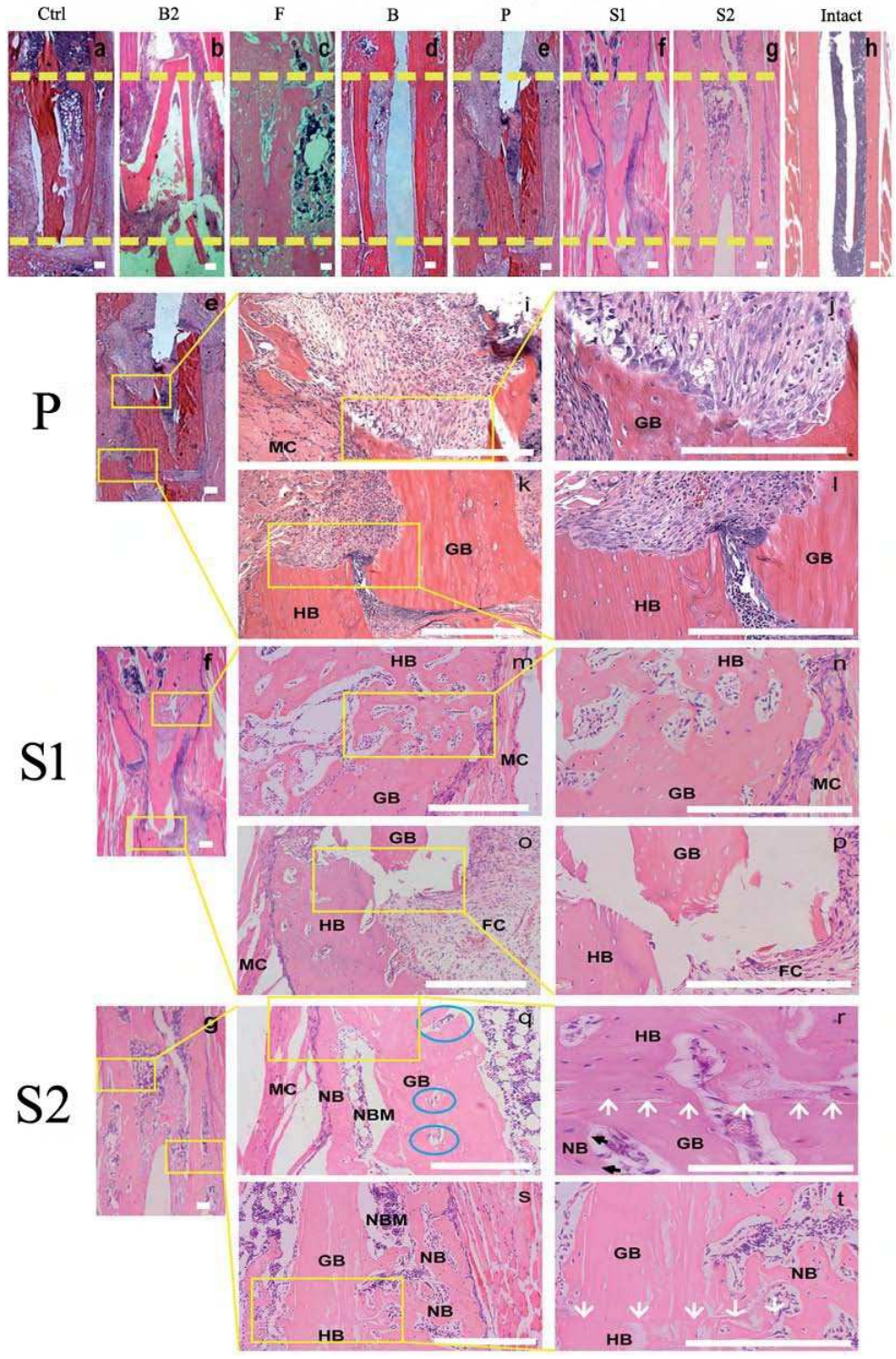

Fig. 19 Histological specimens from hematoxylin-eosin stained micrographs of rat tibiae after 4 weeks of different treatments, with intact contralateral tibiae (left tibiae) and bone fragments without a treatment as the positive and negative controls, respectively. The yellow dotted lines, blue circles and white arrows indicate the original cuts, lacunae with active osteocytes and bone union with host tibia, respectively. HB, GB, FC, NB, NBM, MC refer to the host bone, graft bone, fibrous callus, new bone, new bone marrow, and muscle tissue, respectively. Scale bar: 0.5 mm (reprinted with permission from Ref. 94. Copyright 2015, Royal Society of

Chemistry, License No. 3671210677399).

Fig. 18 shows the soft X-ray photographs of bone bridging after 4 weeks of different treatments. In contrast to the sharp bone ends in group C (**Fig. 18b**) and group B2 (**Fig. 18c**), evident bone bridging was found in group S2 (**Fig. 18h**) after 4 weeks implantation. The hematoxylin-eosin staining micrographs (see **Fig. 19)** showed more details of the histological changes in the bone grafts. There were four perfect contacts between the bone grafts and intact tibia without any gaps (**Fig. 19g, r and t**). In addition, the lacunae with mature osteocytes filled in were observed in the blue circles marked in **Fig. 19q**. However, there was no significant bone bridging in other groups. These *in vivo* observations of group S2 is in accordance with the *in vitro* results presented in **Fig. 17**. Consequently, owing to the controlled release of FGF-2 followed by BMP-2, the core-shell microspheres (with BMP-2 and FGF-2 in core and shell, respectively) would efficiently heal the bone fractures and remodel the bone graft by maintaining the balance between bone formation and resorption.

5. Discussion

As stated above, cell homing-based tissue regeneration can be enhanced by improving the components of tissue engineering triad via cell surface modification, scaffold optimization, and spatiotemporal organization of signaling molecules. Each of these strategies possesses pros and cons, and each of them can be applied individually or in combination for different applications

Cell membranes play key roles in many cellular activities, including cell adhesion, migration and intercellular interactions.[96-100] So cell surface modification via either physical methods or chemical techniques is a promising way to improve cell adhesion and migration during cell homing. However, cell surface modification requires *ex vivo* proliferation of cells, which may result in some problems. For instance, methylation patterns of the cells after removed from their native atmosphere and expanded *ex vivo* may change, leading to the changes in gene expression and cell behavior.[101] Besides, albeit *ex vivo* proliferated cells are not suspected to suffer from a growth deregulation

in vivo, the artificial culture conditions might advantage malignant cells.[102, 103]

The final goal of the tissue engineering scaffold is to replace the natural extracellular matrix (ECM) until cells can rebuild a new natural matrix. To fulfill this goal, scaffold should be not only biocompatible, but also bioactive, which relies on the 3-D structure of the scaffold and the cell-scaffold interactions.[30] As stated in Section 3, the optimization of scaffold can significantly improve cell migration and infiltration in cell homing-based tissue engineering, since the well-ordered structure of scaffolds can obtain proper pore size distribution and porosity. Nevertheless, they are still non-living materials that can hardly react to changes in their atmosphere *in vivo*. In addition, scaffolds made from biomaterials may cause immunological reactions, e.g., fibroblastic overgrowth or rejection, which have negative influence on the final therapeutic outcomes.[104] Due to these limitations, although many engineered tissue scaffold with various structures have been successfully developed for cell homing-based tissue regeneration, a clinically applicable scaffold is still far from being realized.[30, 105, 106]

During the complex wound healing cascade, GFs play a key role in stimulating endogenous repair mechanisms by transferring information to cells and thereby accelerating the functional restoration of defective tissues.[4] Various GFs exert different biological functions in cell homing-based tissue engineering, including improving cell adhesion, proliferation and differentiations. Since a cocktail application of various GFs probably leads to potentially negative effects on tissue repair, there is a consensus that a spatiotemporal delivery of GFs is essentially required for an efficient tissue repair. However, the complexity of the physiological and pathological environments in tissues makes it difficult to figure out a simplified version of the spatiotemporal patterns of the GFs of interest. As a result, it is difficult for materials scientists to design delivery systems for spatiotemporal delivery of these GFs *in situ*.[2] Moreover, although some studies claimed that the introduction of GFs to scaffolds or tissue defects apparently improved the cell homing-based tissue regeneration, the concentrations and profiles of the GFs are warranted to be optimized

for clinical applications. In this regard, the study of spatiotemporal delivery of multiple GFs is still at its infant stage.[107, 108]

6. Conclusion

This work aims at the understanding of the roles of materials in cell homing-based tissue regeneration. Various techniques, which can improve cell migration, adhesion, infiltration, proliferation or differentiation, have been reviewed from the aspect of material science. These techniques focus not only on the modification of cells, but also on the design of scaffolds for cell recruitment, the selection and coordinated release of GFs in situ.

Surface modification of cells using polymers is an important strategy to improve cell homing from the materials' point of view. After introducing a receptor on cell surface, the cell homing efficiency can be obviously enhanced. Besides cell surface modification, the morphology and microstructures of scaffolds can be optimized to improve cell migration and infiltration. In this case, the ordered structures show better performance than the random ones. In addition, a scaffold enabling releasing multiple GFs in specific temporal patterns may help improve the efficiency of coordinating cell proliferation and differentiations. Scaffold optimization in terms of scaffold microstructures and release properties aims at taking full advantage of the cells homed via the technique of cell surface modifications.

Although a series of progress on cell surface modification and scaffold design have been achieved and made biomaterials preparation for cell homing-based tissue regeneration, cell homing-based tissue regeneration is still in its infant stage. As a new strategy for tissue regeneration, cell homing is yet to be better understood and a foreseeable bottleneck is the *in vivo* monitoring of cell homing to defect site and the actual role of these cells in tissue regeneration. These investigations would enable us to understand more about the role of different cells (transplanted and endogenous cells) in regeneration and determine the optimal regenerative approach. After all,

regeneration is the end and cell homing is the means. It is expected that the development of biomaterials would continue to play a big role in solving the bottleneck problems related to cell homing-based tissue regeneration in the future.

Acknowledgments

This work was funded by the Growth Fund for Young Teacher (531107040850, D. Zhao), the Hunan Provincial Science and Technology Program (2014FJ6031, L. Lei), the Hunan Provincial Science Found for Distinguished Young Scholars (2015JJ1007, H. Nie), and the National Natural Science Foundation of China (31200727, H. Nie). The authors wish to confirm that there are no known conflicts of interest associated with this publication.

References

1. C. H. Lee, J. L. Cook, A. Mendelson, E. K. Moioli, H. Yao and J. J. Mao, *Lancet*, 2010, 376, 440-448.
2. F.-M. Chen, M. Zhang and Z.-F. Wu, *Biomaterials*, 2010, 31, 6279-6308.
3. F.-M. Chen, J. Zhang, M. Zhang, Y. An, F. Chen and Z.-F. Wu, *Biomaterials*, 2010, 31, 7892-7927.
4. M. Biondi, F. Ungaro, F. Quaglia and P. A. Netti, *Advanced Drug Delivery Reviews*, 2008, 60, 229-242.
5. I. Drosse, E. Volkmer, R. Capanna, P. D. Biase, W. Mutschler and M. Schieker, *Injury*, 2008, 39, Supplement 2, S9-S20.
6. D. W. Hutmacher, *Biomaterials*, 2000, 21, 2529-2543.
7. G. T. Huang, M. Al-Habib and P. Gauthier, *Endod Topics*, 2013, 28, 51-60.
8. J. E. Schroeder and R. Mosheiff, *Injury*, 2011, 42, 609-613.
9. P. N. Soucacos, E. O. Johnson and G. Babis, *Injury*, 2008, 39, Supplement 2, S1-S4.
10. S. B. Goodman, *Minerva Ortop Traumatol*, 2013, 64, 107-113.
11. Y. Gong, Y. Zhao, Y. Li, Y. Fan and J. Hoover-Plow, *Journal of the American College of Cardiology*, 2014, 63, 2862-2872.
12. F. Di Scipio, A. E. Sprio, A. Folino, M. E. Carere, P. Salamone, Z. Yang, M. Berrone, M. Prat, G. Losano, R. Rastaldo and G. N. Berta, *Biochimica et Biophysica Acta (BBA) - General Subjects*, 2014, 1840, 2152-2161.
13. C. Kyriakou, N. Rabin, A. Pizzey, A. Nathwani and K. Yong, *Haematologica*, 2008, 93, 1457-1465.
14. K. Dashnyam, R. Perez, E.-J. Lee, Y.-R. Yun, J.-H. Jang, I. B. Wall and H.-W. Kim, *Journal of Biomedical Materials Research Part A*, 2014, 102, 1859-1867.
15. C.-H. Lee, M. U. Jin, H.-M. Jung, J.-T. Lee and T.-G. Kwon, *PLoS ONE*, 2015, 10, e0120051.
16. Y.-S. Liu, M.-E. Ou, H. Liu, M. Gu, L.-W. Lv, C. Fan, T. Chen, X.-H. Zhao, C.-Y. Jin, X. Zhang, Y. Ding and Y.-S. Zhou, *Biomaterials*, 2014, 35, 4489-4498.

17. D. Chanda, S. Kumar and S. Ponnazhagan, *Journal of Cellular Biochemistry*, 2010, 111, 249-257.
18. R. F. Wynn, C. A. Hart, C. Corradi-Perini, L. O'Neill, C. A. Evans, J. E. Wraith, L. J. Fairbairn and I. Bellantuono, *A small proportion of mesenchymal stem cells strongly expresses functionally active CXCR4 receptor capable of promoting migration to bone marrow*, 2004.
19. D. G. Phinney and D. J. Prockop, *Stem Cells*, 2007, 25, 2896-2902.
20. R. Sackstein, J. S. Merzaban, D. W. Cain, N. M. Dagia, J. A. Spencer, C. P. Lin and R. Wohlgemuth, *Nat Med*, 2008, 14, 181-187.
21. Y. Teramura and H. Iwata, *Soft Matter*, 2010, 6, 1081-1091.
22. D. Sarkar, J. A. Spencer, J. A. Phillips, W. Zhao, S. Schafer, D. P. Spelke, L. J. Mortensen, J. P. Ruiz, P. K. Vemula and R. Sridharan, *Blood*, 2011, 118.
23. V. Gribova, T. Crouzier and C. Picart, *Journal of Materials Chemistry*, 2011, 21, 14354-14366.
24. R. A. Perez and H.-W. Kim, *Acta Biomaterialia*, 2015, 21, 2-19.
25. D. Rana, S. Arulkumar, A. Vishwakarma and M. Ramalingam, in *Stem Cell Biology and Tissue Engineering in Dental Sciences*, ed. A. V. S. S. Ramalingam, Academic Press, Boston, 2015, DOI: http://dx.doi.org/10.1016/B978-0-12-397157-9.00012-6, pp. 133-148.
26. J. C. Dinis, T. F. Morais, P. H. J. Amorim, R. B. Ruben, H. A. Almeida, P. N. Inforçati, P. J. Bártolo and J. V. L. Silva, *Procedia Technology*, 2014, 16, 1542-1547.
27. S. M. Giannitelli, D. Accoto, M. Trombetta and A. Rainer, *Acta Biomaterialia*, 2014, 10, 580-594.
28. K. Kim, C. H. Lee, B. K. Kim and J. J. Mao, *J Dent Res*, 2010, 89, 842-847.
29. P. Newham and M. J. Humphries, *Molecular Medicine Today*, 1996, 2, 304-313.
30. H. Chen, Y. Liu, Z. Jiang, W. Chen, Y. Yu and Q. Hu, *Experimental Cell Research*, 2014, 323, 346-351.
31. J. R. Mauney and R. M. Adam, *Advanced Drug Delivery Reviews*, 2015, 82–83, 77-85.
32. B. G. Sengers, M. Taylor, C. P. Please and R. O. C. Oreffo, *Biomaterials*, 2007, 28, 1926-1940.
33. H.-H. Sun, T.-J. Qu, X.-H. Zhang, Q. Yu and F.-M. Chen, *Biotechnology Progress*, 2012, 28, 3-20.
34. B. Boilly, A. S. Vercoutter-Edouart, H. Hondermarck, V. Nurcombe and X. Le Bourhis, *Cytokine Growth Factor Rev*, 2000, 11, 295-302.
35. L. R. Chaudhary, A. M. Hofmeister and K. A. Hruska, *Bone*, 2004, 34, 402-411.
36. J. G. Pickering, S. Uniyal, C. M. Ford, T. Chau, M. A. Laurin, L. H. Chow, C. G. Ellis, J. Fish and B. M. Chan, *Circ Res*, 1997, 80, 627-637.
37. P. J. Marie, F. Debiais and E. Hay, *Histol Histopathol*, 2002, 17, 877-885.
38. T. J. Cho, L. C. Gerstenfeld and T. A. Einhorn, *J Bone Miner Res*, 2002, 17, 513-520.
39. C. Laflamme and M. Rouabhia, *Biomed Mater*, 2008, 3, 015008.
40. I. Pountos, T. Georgouli, K. Henshaw, H. Bird, E. Jones and P. V. Giannoudis, *J Orthop Trauma*, 2010, 24, 552-556.
41. D. H. Kempen, L. Lu, A. Heijink, T. E. Hefferan, L. B. Creemers, A. Maran, M. J. Yaszemski and W. J. Dhert, *Biomaterials*, 2009, 30, 2816-2825.
42. I. Martin, R. Suetterlin, W. Baschong, M. Heberer, G. Vunjak-Novakovic and L. E. Freed, *J Cell Biochem*, 2001, 83, 121-128.
43. P. Yilgor, N. Hasirci and V. Hasirci, *J Biomed Mater Res A*, 2010, 93, 528-536.
44. W. J. King and P. H. Krebsbach, *Advanced Drug Delivery Reviews*, 2012, 64, 1239-1256.

45. J. A. Jansen, J. W. M. Vehof, P. Q. Ruhé, H. Kroeze-Deutman, Y. Kuboki, H. Takita, E. L. Hedberg and A. G. Mikos, *Journal of Controlled Release*, 2005, 101, 127-136.
46. F.-M. Chen, L.-A. Wu, M. Zhang, R. Zhang and H.-H. Sun, *Biomaterials*, 2011, 32, 3189-3209.
47. Q. Wang, H. Cheng, H. Peng, H. Zhou, P. Y. Li and R. Langer, *Advanced Drug Delivery Reviews*, 2014, DOI: http://dx.doi.org/10.1016/j.addr.2014.12.003.
48. F.-M. Chen, H.-H. Sun, H. Lu and Q. Yu, *Biomaterials*, 2012, 33, 6320-6344.
49. J. S. Temenoff and A. G. Mikos, *Biomaterials*, 2000, 21, 431-440.
50. R. Sackstein, *Ann Biomed Eng*, 2012, 40, 766-776.
51. Y. Imai, M. S. Singer, C. Fennie, L. A. Lasky and S. D. Rosen, *The Journal of Cell Biology*, 1991, 113, 1213-1221.
52. A. T. Askari, S. Unzek, Z. B. Popovic, C. K. Goldman, F. Forudi, M. Kiedrowski, A. Rovner, S. G. Ellis, J. D. Thomas, P. E. DiCorleto, E. J. Topol and M. S. Penn, *The Lancet*, 2003, 362, 697-703.
53. Y. L. Tang, K. Qian, Y. C. Zhang, L. Shen and M. I. Phillips, *Regulatory Peptides*, 2005, 125, 1-8.
54. A. Bajetto, F. Barbieri, A. Dorcaratto, S. Barbero, A. Daga, C. Porcile, J. L. Ravetti, G. Zona, R. Spaziante, G. Corte, G. Schettini and T. Florio, *Neurochemistry International*, 2006, 49, 423-432.
55. Y. Teramura, *Biomaterials*, 2015, 48, 119-128.
56. Y. Teramura, Y. Kaneda, T. Totani and H. Iwata, *Biomaterials*, 2008, 29, 1345-1355.
57. Y. W. Won, A. N. Patel and D. A. Bull, *Biomaterials*, 2014, 35, 5627-5635.
58. L.-T. Chang, C.-M. Yuen, C.-K. Sun, C.-J. Wu, J.-J. Sheu, S. Chua, K.-H. Yeh, C.-H. Yang, A. A. Youssef and H.-K. Yip, *Circulation Journal*, 2009, 73, 1097-1104.
59. M. Kucia, B. Dawn, G. Hunt, Y. Guo, M. Wysoczynski, M. Majka, J. Ratajczak, F. Rezzoug, S. T. Ildstad, R. Bolli and M. Z. Ratajczak, *Circulation Research*, 2004, 95, 1191-1199.
60. D. Wong and W. Korz, *Clinical Cancer Research*, 2008, 14, 7975-7980.
61. J. E. Jeon, C. Vaquette, C. Theodoropoulos, T. J. Klein and D. W. Hutmacher, *Multiphasic construct studied in an ectopic osteochondral defect model*, 2014.
62. D. Zhao, K. Chang, T. Ebel, M. Qian, R. Willumeit, M. Yan and F. Pyczak, *Journal of the Mechanical Behavior of Biomedical Materials*, 2013, 28, 171-182.
63. H. A. Almeida and P. J. Bártolo, *Procedia Engineering*, 2013, 59, 298-306.
64. B. J. C. Luthringer, F. Ali, H. Akaichi, F. Feyerabend, T. Ebel and R. Willumeit, *Journal of Materials Science: Materials in Medicine*, 2013, 24, 2337-2358.
65. J. X. Lu, B. Flautre, K. Anselme, P. Hardouin, A. Gallur, M. Descamps and B. Thierry, *Journal of Materials Science: Materials in Medicine*, 1999, 10, 111-120.
66. V. Karageorgiou and D. Kaplan, *Biomaterials*, 2005, 26, 5474-5491.
67. D. Zhao, K. Chang, T. Ebel, H. Nie, R. Willumeit and F. Pyczak, *Journal of Alloys and Compounds*, 2015, 640, 393-400.
68. W. Zhao, B. Yalcin and M. Cakmak, *Synthetic Metals*, 2015, 203, 107-116.
69. B. Sun, X.-J. Jiang, S. Zhang, J.-C. Zhang, Y.-F. Li, Q.-Z. You and Y.-Z. Long, *Journal of Materials Chemistry B*, 2015, 3, 5389-5410.
70. A. R. Unnithan, R. S. Arathyram and C. S. Kim, in *Nanotechnology Applications for Tissue Engineering*, ed. S. T. G. Ninan, William Andrew Publishing, Oxford, 2015, DOI: http://dx.doi.org/10.1016/B978-0-323-32889-0.00003-0, pp. 45-55.
71. S. Wang, S. Zhong, C. T. Lim and H. Nie, *Journal of Materials Chemistry B*, 2015.
72. P. Chen, J. Tao, S. Zhu, Y. Cai, Q. Mao, D. Yu, J. Dai and H. Ouyang, *Biomaterials*, 2015, 39,

114-123.

73. H. D. Theiss, M. Vallaster, C. Rischpler, L. Krieg, M.-M. Zaruba, S. Brunner, Y. Vanchev, R. Fischer, M. Gröbner, B. Huber, T. Wollenweber, G. Assmann, J. Mueller-Hoecker, M. Hacker and W.-M. Franz, *Stem Cell Research*, 2011, 7, 244-255.
74. J. Y. Park, J.-H. Shim, S.-A. Choi, J. Jang, M. Kim, S. H. Lee and D.-W. Cho, *Journal of Materials Chemistry B*, 2015, 3, 5415-5425.
75. B. Starly and R. Shirwaiker, in *3D Bioprinting and Nanotechnology in Tissue Engineering and Regenerative Medicine*, eds. L. G. Zhang, J. P. Fisher and K. W. Leong, Academic Press, 2015, DOI: http://dx.doi.org/10.1016/B978-0-12-800547-7.00003-5, pp. 57-77.
76. K. F. Leong, D. Liu and C. K. Chua, in *Comprehensive Materials Processing*, ed. S. H. F. B. J. V. T. Yilbas, Elsevier, Oxford, 2014, DOI: http://dx.doi.org/10.1016/B978-0-08-096532-1.01010-4, pp. 251-264.
77. M. Asadi-Eydivand, M. Solati-Hashjin, A. Farzad and N. A. Abu Osman, *Robotics and Computer-Integrated Manufacturing*, 2016, 37, 57-67.
78. S. C. Cox, J. A. Thornby, G. J. Gibbons, M. A. Williams and K. K. Mallick, *Materials Science and Engineering: C*, 2015, 47, 237-247.
79. R. Gaetani, D. A. M. Feyen, V. Verhage, R. Slaats, E. Messina, K. L. Christman, A. Giacomello, P. A. F. M. Doevendans and J. P. G. Sluijter, *Biomaterials*, 2015, 61, 339-348.
80. G. Gagg, E. Ghassemieh and F. E. Wiria, *Materials Science and Engineering: C*, 2013, 33, 3858-3864.
81. S. Maleksaeedi, J. K. Wang, A. El-Hajje, L. Harb, V. Guneta, Z. He, F. E. Wiria, C. Choong and A. J. Ruys, *Procedia CIRP*, 2013, 5, 158-163.
82. S. Mohanty, L. B. Larsen, J. Trifol, P. Szabo, H. V. R. Burri, C. Canali, M. Dufva, J. Emnéus and A. Wolff, *Materials Science and Engineering: C*, 2015, 55, 569-578.
83. M. Xu, H. Li, D. Zhai, J. Chang, S. Chen and C. Wu, *Journal of Materials Chemistry B*, 2015, 3, 3799-3809.
84. M. Xu, D. Zhai, J. Chang and C. Wu, *Acta Biomaterialia*, 2014, 10, 463-476.
85. T. Orita, M. Tomita and K. Kato, *Colloids and Surfaces B: Biointerfaces*, 2011, 84, 187-197.
86. M. Chatzinikolaidou, S. Rekstyte, P. Danilevicius, C. Pontikoglou, H. Papadaki, M. Farsari and M. Vamvakaki, *Materials Science and Engineering: C*, 2015, 48, 301-309.
87. G. R. Mitchell and A. Tojeira, *Procedia Engineering*, 2013, 59, 117-125.
88. M. A. LaBarge and H. M. Blau, *Cell*, 2002, 111, 589-601.
89. H. Nie, Z. Dong, D. Y. Arifin, Y. Hu and C.-H. Wang, *Journal of Biomedical Materials Research Part A*, 2010, 95A, 709-716.
90. K. Whitehead, Z. Shen and S. Mitragotri, *Journal of Controlled Release*, 2004, 98, 37-45.
91. J. Kim, J. E. Lee, S. H. Lee, J. H. Yu, J. H. Lee, T. G. Park and T. Hyeon, *Advanced Materials*, 2008, 20, 478-483.
92. H. Nie, Y. Fu and C.-H. Wang, *Biomaterials*, 2010, 31, 8732-8740.
93. L. Lei, S. Wang, H. Wu, W. Ju, J. Peng, A. S. Qahtan, C. Chen, Y. Lu, X. Zhang and H. Nie, *J Biomed Mater Res A*, 2015, 103, 252-261.
94. S. Wang, W. Ju, P. Shang, L. Lei and H. Nie, *Journal of Materials Chemistry B*, 2015.
95. I. Martin, R. Suetterlin, W. Baschong, M. Heberer, G. Vunjak-Novakovic and L. E. Freed, *Journal of Cellular Biochemistry*, 2001, 83, 121-128.
96. M. Kato and M. Mrksich, *Journal of the American Chemical Society*, 2004, 126, 6504-6505.

97. A. D. Luster, R. Alon and U. H. von Andrian, *Nat Immunol*, 2005, 6, 1182-1190.
98. A. Mantovani, P. Allavena, A. Sica and F. Balkwill, *Nature*, 2008, 454, 436-444.
99. J. M. Karp and G. S. Leng Teo, *Cell Stem Cell*, 2009, 4, 206-216.
100. Q. Shen, Y. Wang, E. Kokovay, G. Lin, S.-M. Chuang, S. K. Goderie, B. Roysam and S. Temple, *Cell Stem Cell*, 2008, 3, 289-300.
101. J. N. Rottman and J. I. Gordon, *Journal of Biological Chemistry*, 1993, 268, 11994-12002.
102. H. Rubin, in *Advances in Cancer Research*, Academic Press, 2001, vol. Volume 83, pp. 159-207.
103. M. E. Bernardo, N. Zaffaroni, F. Novara, A. M. Cometa, M. A. Avanzini, A. Moretta, D. Montagna, R. Maccario, R. Villa, M. G. Daidone, O. Zuffardi and F. Locatelli, *Cancer Research*, 2007, 67, 9142-9149.
104. J. M. Kelm and M. Fussenegger, *Advanced Drug Delivery Reviews*, 2010, 62, 753-764.
105. Z. Xiong, Y. Yan, S. Wang, R. Zhang and C. Zhang, *Scripta Materialia*, 2002, 46, 771-776.
106. L. Moroni, J. R. de Wijn and C. A. van Blitterswijk, *Biomaterials*, 2006, 27, 974-985.
107. T. J. Blokhuis, *Injury*, 2009, 40, Supplement 3, S8-S11.
108. V. Alt and A. Heissel, *Current Medical Research and Opinion*, 2006, 22, S19-S22.

Biography & photograph

Dapeng Zhao received his BS and MS in Materials Science and Engineering from Central South University (China) in 2008 and 2010, respectively, and PhD degree in Materials Science from the Brandenburg University of Technology Cottbus-Senftenberg (Germany) in 2014. At present, he is an assistant professor in Prof. Hemin Nie's group at the Department of Biomedical Engineering, Hunan University (China). His current research interests are primarily in titanium and magnesium based materials for biomedical applications.

Lei Lei received her BDS, MDS and DDS from Xiangya Medical School of Central South University (China) in 2008, 2011 and 2014, respectively. She is currently an attending physician at the Department of Orthodontics of Xiangya Stomatological Hospital, Central South University (China). Her current research interests are primarily in orthodontic tooth movement, tooth regeneration and bone regeneration.

Shuo Wang received his BS in Life Science from Hunan Agricultural University (China) in 2006, and MS in Biochemistry and Molecular Biology from Hunan Normal University (China) in 2009. He is currently a PhD candidate in Prof. Hemin Nie's group at the Department of Biomedical Engineering, Hunan University (China). His current research is focused on the development of biomaterials for cell homing-based bone regeneration.

Hemin Nie received his PhD in Chemical and Biomolecular Engineering from National University of Singapore in 2009. Afterwards, he moved to Columbia University in the City of New York as a postdoctoral fellow and continued his research on biomaterials and controlled-release techniques in the interest of tissue engineering and regenerative medicine. He is currently a professor at the Department of Biomedical Engineering, Hunan University (China). His research interests include cell-transplantation and cell homing for tissue regeneration, controlled-release techniques, and the applications of biomaterials in regenerative medicine.

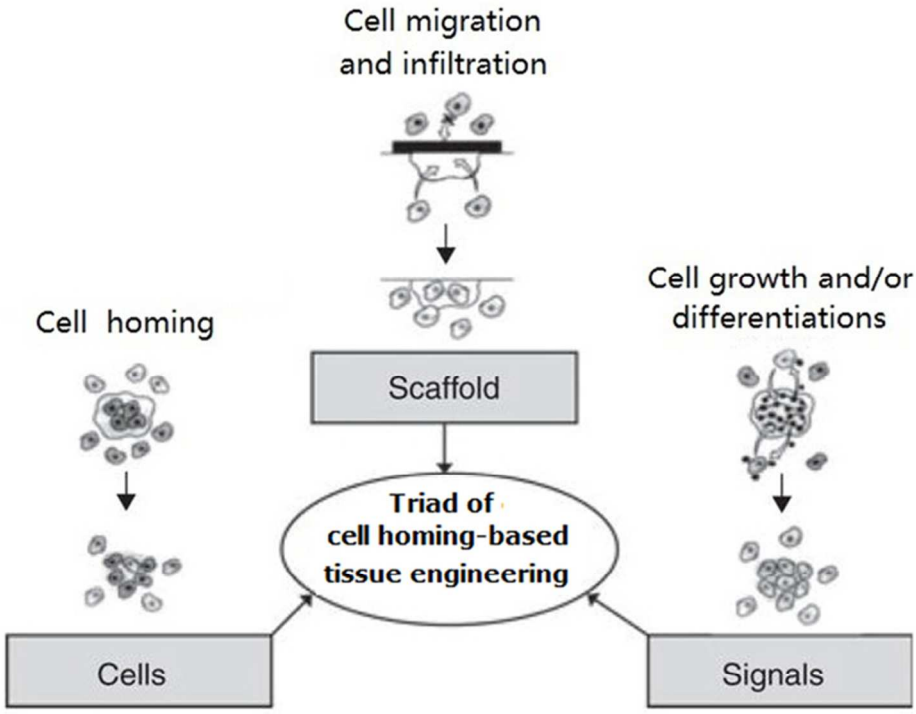

The Triad of Cell Homing-Based Tissue Engineering.
63x50mm (300 x 300 DPI)